Absorption cross section and signal enhancement in Er-doped Si nanocluster rib-loaded waveguides

N. Daldosso,[a] D. Navarro-Urrios, M. Melchiorri, and L. Pavesi
Dipartimento di Fisica, Università di Trento, Via Sommarive 14, I-38050 Povo (Trento), Italy

F. Gourbilleau, M. Carrada, and R. Rizk
SIFCOM, UMR CNRS 6176, ENSICAEN, 6 Boulevard Maréchal Juin, 14050 CAEN, France

C. García, P. Pellegrino, and B. Garrido
EME, Department d' Electrònica, Universitat de Barcelona, Martí i Franquès, 1, 08028 Barcelona, Spain

L. Cognolato
Agilent Technologies, Via G. ReissRomoli 274, I-10148 Torino, Italy

(Received 1 November 2004; accepted 17 May 2005; published online 20 June 2005)

Pump and probe experiments on Er^{3+} ions coupled to Si nanoclusters have been performed in rib-loaded waveguides to investigate optical amplification at 1.5 μm. Rib-loaded waveguides were obtained by photolithographic and reactive ion etching of Er-doped silica layers containing Si nanoclusters grown by reactive sputtering. Insertion losses measurements in the infrared erbium absorption region allowed to gauge an Er^{3+} absorption cross section of about 5×10^{-21} cm^2 at 1534 nm. Signal transmission under optical pumping at 1310 nm shows confined carrier absorption of the Si nanoclusters. Amplification experiments at 1535 nm evidence two pump power regimes: Losses due to confined carrier absorption in the Si nanoclusters at low pump powers and signal enhancement at high pump powers. For strong optical pumping, signal enhancement of about 1.2 dB/cm was obtained. © *2005 American Institute of Physics*. [DOI: 10.1063/1.1957112]

To develop on-chip optical amplifier, Er^{3+}-doped planar glass optical amplifier operating at 1.5 μm are actively looked for. Compact amplifiers at 1535 nm with a gain value of about 2–4 dB/cm have been demonstrated.[1,2] However, these systems have both an intrinsic limit, e.g., cooperative upconversion and excited state absorption, and extrinsic limit, e.g., the need for expensive 980 nm or 1480 nm pump lasers. The use of suitable Er^{3+} sensitizers could overcome these limitations.[3] Si nanoclusters (Si-nc) in SiO_2 are good candidates[4] because of their broad and continuous absorption band in the visible and of the possibility of electrical excitation.[5] Excitation is transferred from the Si-nc to the Er^{3+} ions via a fast ($\sim$1 μs), very efficient ($>$70%), and with a large excitation cross section ($\sim10^{-16}$ cm^2 at 488 nm) process.[4]

Encouraging results on Er^{3+}-Si-nc coupled waveguides have been published. A large internal gain by light emitting diode pumping and an unexpectedly high emission cross section for Er^{3+} ($\sigma_{em}\sim2\times10^{-19}$ cm^2 at 1535 nm) were found.[6] Another work reported on an enhanced absorption cross section $\sigma_{abs}\sim8\times10^{-20}$ cm^2 at 1535 nm.[7] Thus, in this letter, we address the problem of light amplification in Er-doped silica rib-loaded waveguides containing Si-nc with the aim to check these cross section values.

Er^{3+} and Si-nc rich waveguides have been prepared by reactive magnetron co-sputtering of a pure silica target topped with Er_2O_3 pellets.[8,9] The incorporation of Si excess in the film was obtained by mixing the plasma with hydrogen, owing to its ability to reduce the oxygen provided by the silica target.[10] The hydrogen rate (mixed to argon) was kept to 60% while the Si substrates, on which a 10 μm thermal SiO_2 layer was previously grown, were not intentionally heated. More details on the process have been given elsewhere.[8,9] After the deposition of a 0.75 μm thick Er/Si-nc rich layer, a 1 μm thick SiO_2 cladding layer was deposited by sputtering a SiO_2 target in a pure argon plasma. Then, the samples were annealed for 1 h at 900 °C under a pure N_2 flux to activate Er^{3+}, form Si nanoclusters, and maximize the energy transfer from the Si-nc to Er^{3+} ions. By the use of secondary ion mass spectroscopy (SIMS) and Rutherford backscattering spectroscopy (RBS), a Si excess of 7 at. % and an Er concentration $N_{Er}\sim4\times10^{20}$ cm^{-3} ($\sim$0.5 at. %) were found. A refractive index n of 1.531 at 1553 nm was determined by m-line measurements. Optical lithography and reactive ion etching have been used to define rib-loaded waveguides with rib widths between 2 and 6 μm (optical confinement factor $\Gamma\sim0.55$). 3 cm long waveguides were used for measurements.

Light from a tuneable laser (1.5–1.6 μm) or a diode laser (1.31 μm) was coupled into the waveguide through a single-mode polarization-preserving tapered fiber moved by a piezoelectric stage. The light exiting the end facet of the waveguide was observed through a prism beam splitter with a microscope objective (40×) matched both to a zoom (2–12×), mounted on an InGaAs camera and to a calibrated Ge detector. For signal amplification measurements, the optical pumping was supplied by an Ar laser (488 nm, up to a power of 2.4 W), focused on the waveguide surface into a stripe 10 μm wide and 0.9 cm long by means of a cylindrical lens. The alignment of the pump with the rib-loaded waveguide was checked by two cameras for side and top observations. Note that only the last 0.9 cm of the 3 cm long rib waveguide was pumped. The probe signal was chopped (10 kHz, 0.2 mW) and detected through a lock in to clean the amplified spontaneous emission from the signal. Propagation losses (α_{prop}) have been determined from insertion

[a]Electronic mail: daldosso@science.unitn.it

TABLE I. Propagation losses coefficients for 6 and 5 μm wide rib-loaded waveguide at different wavelengths.

λ (nm)	α (dB/cm) 6 μm width	α (dB/cm) 5 μm width
1310	<6	<6
1500	<4.5	<4.5
1534	<7	<7
1550	<3.5	<3.5
1600	<2	<2

losses measurements once the coupling losses have been estimated (about 10 dB) both by calculations and by comparison with similar waveguides in which propagation losses have been measured independently.[11]

In Table I, α_{prop} for unpolarized light at different wavelengths are shown. No significant differences for the transverse electric and transverse magnetic modes have been observed. The difference between α_{prop} at 1534 and 1600 nm is due to the different strength of the Er^{3+} absorption α_{Er} and to the wavelength dependence of scattering losses. By assuming a negligible α_{Er} at 1600 nm and a smooth variation of the Rayleigh scattering loss in the 1500–1600 nm wavelength region, we can subtract from α_{prop} the scattering losses and, thus, estimate α_{Er}. In Fig. 1 (dotted line) α_{Er} is reported and compared to the luminescence spectrum. $\alpha_{Er}=\Gamma\sigma_{abs}N_{Er}$ is about 4.8 dB/cm at 1534 nm, which corresponds to a peak $\sigma_{abs}\sim 5\pm 2\times 10^{-21}$ cm^2. Note that here we have assumed that all the Er is optically active. This value coincides with that of Er^{3+} in pure silica[12] and contrasts to that measured in Ref. 7. Ion implantation, a larger Si excess (13 at. %), a smaller Γ factor and a higher annealing temperature were used in Ref. 7.

The Si-nc acted as Er^{3+} sensitizers in our waveguides as evidenced in Ref. 9, where an Er^{3+} excitation cross sections $\sigma_{exc}\sim 5\times 10^{16}$ cm^2 at 457 nm was measured at low photon flux ($\Phi\sim 10^{16}$–10^{17} photon/s cm^2). This is also shown in Fig. 2, where the Er^{3+} emission intensity as a function of Φ for both resonant (488 nm) and nonresonant (476 nm) pumping is reported. For $\phi<10^{19}$ photons/s cm^2, resonant and nonresonant pumping yields the same emission intensity, which implies efficient energy transfer. At Φ

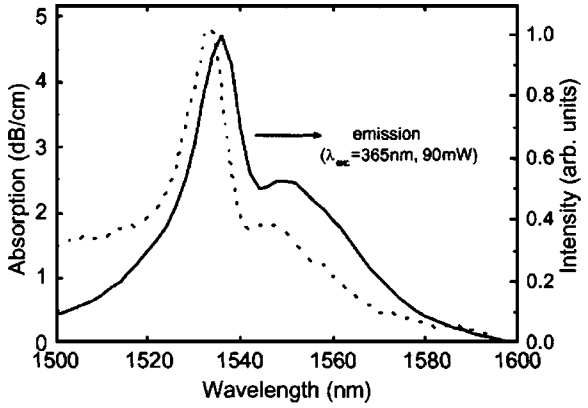

FIG. 1. Emission (full line) and absorption (dotted line) spectra of Er-doped Si nanoclusters waveguide. The emission spectrum is obtained with an excitation wavelength of 365 nm and excitation power of 90 mW, luminescence is collected from the waveguide facet. The absorption spectrum is obtained by measuring the insertion losses as a function of the wavelength. Room-temperature measurements.

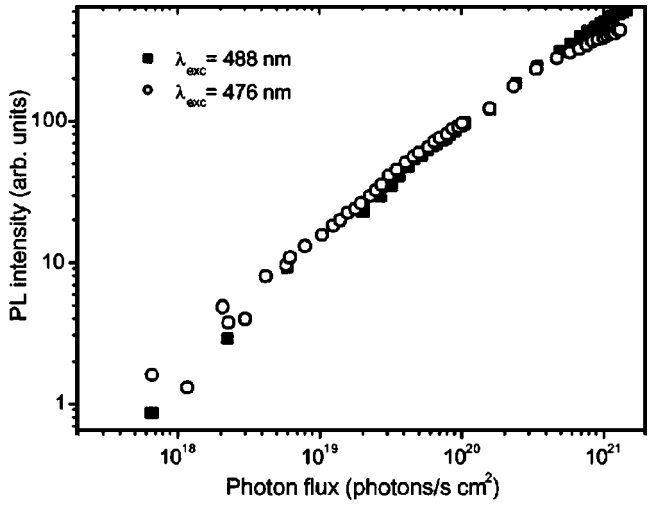

FIG. 2. Luminescence intensity at 1535 nm as a function of the photon flux for resonant (488 nm) and nonresonant (476 nm) excitations. Room-temperature measurements.

$>10^{20}$ photons/s cm^2, emission for resonant pumping is larger than for nonresonant pumping due to a saturation of the Si-nc excitation:[13] Direct excitation of Er^{3+} becomes more efficient than indirect excitation through the Si-nc, probably because not all of the active Er ions are coupled to the Si-nc. No Φ-dependence of the Er^{3+} emission decay time ($\sim$3.9 ms) has been observed,[14] suggesting that both Auger cooperative Er upconversion and excited state absorption are negligible. It is worth noting that the linear increase of the PL intensity as a function of the 488 nm pump power suggests that the population of Er^{3+} excited state is increasing with the photon flux.

Amplification measurements are reported in Fig. 3. The transmitted signal intensity under optical pumping I_{pump} can be approximated by $I_{pump}=I_{probe}\exp[2(\Gamma\sigma_{em}N_{Er}^{*})L]$,[6] where I_{probe} is the transmitted signal intensity without optical pumping, N_{Er}^{*} is the density of excited Er^{3+}, and L is the length of

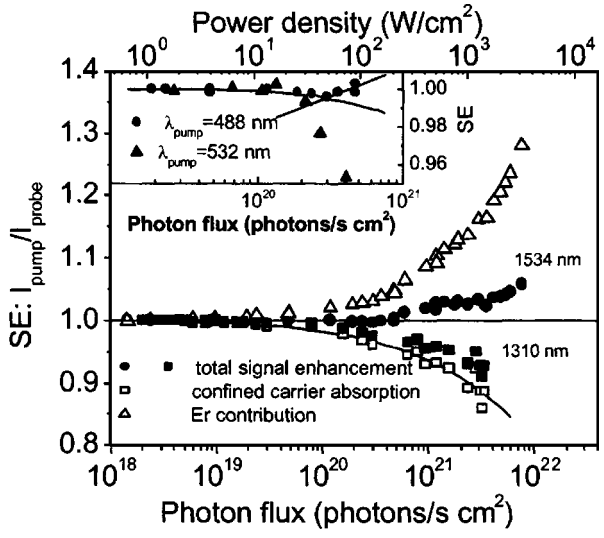

FIG. 3. SE at 1534 nm (disks) and at 1310 nm (filled squares) as a function of the 488 nm photon flux. Empty squares and triangles refer to the contribution to SE at 1534 nm due to confined carrier absorption and Er^{3+} amplification, respectively. The inset reports a blow-up of the SE at 1534 nm for photon flux of 10^{19}–10^{21} photons/s cm^2 (the lines act as guides for the eyes) and for two different pump wavelengths (488 nm disks and 532 nm triangles).

the optically pumped region of the waveguide; hence, the signal enhancement $SE = I_{pump}/I_{probe}$. At 1310 nm, where Er^{3+} is not active, SE decreases with increasing Φ (filled squares in Fig. 3). We attribute the SE decrease to absorption of the signal light by excited carriers confined within the Si-nc.[15] By considering as carrier absorption cross section that of bulk Si (about 7×10^{-18} cm^2 at 1.5 μm),[16] the data can be adequately fitted. Two trends are clear in the Φ-dependence of SE at 1534 nm (disks in Fig. 3). For low Φ (i.e., $\Phi<4\times10^{20}$ photons/s cm^2), a behavior similar to the one observed at 1310 nm is measured (see inset in Fig. 3), i.e., confined carrier absorption dominates. Note that the data reported in Ref. 7 refers to this low pumping regime. For higher Φ, signal enhancement of about 1.06 is observed for $\Phi\sim6\times10^{21}$ photons/s cm^2. $SE>1$ has been observed only in the 1530–1540 nm range. Note that when the pump wavelength is 532 nm, we do not measure any SE (see inset in Fig. 3).

The data reported in the inset of Fig. 3, where a region of negative SE is observed, show that the two processes (Si-nc confined carrier absorption and Er^{3+}-related signal enhancement) can be considered additive and that signal enhancement is only observed when the pump wavelength is resonant with an Er^{3+} internal transition. Considering that the free-carrier absorption cross section $\sigma_{fc}(1.54\ \mu m)\sim1.6\sigma_{fc}(1.32\ \mu m)$ in Si,[17] we extrapolate the contribution to SE of confined carrier absorption at 1.534 μm from the 1.31 μm SE data: $SE_{cc}(1.54\ \mu m)\sim[SE(1.3\ \mu m)]^{1.6}$ (open squares in Fig. 3). Then by using SE_{cc}, one can isolate the Er^{3+}-related contribution to SE (triangles in Fig. 3). It is worth noting that confined carrier absorption not only has the effect of introducing a loss mechanism but also of turning off the indirect channel of Er^{3+} excitation, so that Er^{3+} can be excited only through direct absorption. Indeed, optically pumping with 457 nm and 532 nm light does not show signal enhancement up to $\Phi=1.4\times10^{20}$ and 5×10^{20} photons/s cm^2, respectively.

By using the model proposed in Ref. 6, the maximum effective SE of 1.28 due to Er^{3+} translates into an internal gain coefficient $g=\Gamma\sigma_{em}N_{Er}\sim0.6$ dB/cm and in a $\sigma_{exc}\sim6\times10^{-21}$ cm^2 at 488 nm. Both numbers are significantly smaller than the ones found in Ref. 6. From the g value and assuming that all the Er is optically active, we could estimate the lower limit of the number of Er ions in the excited state N^*_{Er}: $g=\Gamma N^*_{Er}\sigma_{em}$ and if $\sigma_{em}=\sigma_{abs}$, we obtain $N^*_{Er}=5\times10^{19}$ cm^{-3}, i.e., about 12.5% of Er^{3+} is in the excited state.

In Ref. 6, a larger $g\sim7$ dB/cm has been reported for a 2.5 μm thick waveguide with only 1 at. % Si excess and 0.03–0.05 at. % of Er ($N_{Er}\sim1-2\times10^{19}$ cm^3). The use of a very low Si excess and of a short annealing time (5 min at 1000 °C) reduced the strength of confined carrier absorption, kept effective the indirect excitation of Er^{3+}, and could explain the high g. From the data, an enhanced $\sigma_{em}\sim2\times10^{-19}$ cm^2 at 1535 nm was deduced, which is surprising.[6] In fact, the σ_{em} is proportional to the inverse of the radiative lifetime τ_{rad} of Er^{3+}: An increase of σ_{em} should correspond to a decrease of τ_{rad}. This was not observed and a luminescence decay time of about 8 ms was reported in Ref. 6.

In conclusion, at high photon fluxes, a sizeable signal enhancement in Er^{3+} coupled to Si-nc waveguides was observed. This effect was not coupled to an enhancement in the Er^{3+} absorption cross section, and was strongly limited by confined carrier absorption. Further optimization of the number of active Er ions coupled to each Si-nc can lead to larger signal enhancement.

The authors thank E. Chierici and E. Emelli for waveguide processing and characterization, and C. Sada for the RBS and SIMS measurements. This work was supported by EC (SINERGIA project). One of the authors (M.C.) thanks the Region Basse Normandie for financial support. Trento was also supported by PAT through the PROFILL project and by FIRB project.

[1] G. N. van den Hoven, A. Polman, C. van Dam, J. W. M. van Uffelen, and M. K. Smit, Appl. Phys. Lett. **68**, 1886 (1996).
[2] Y. C. Yan, A. J. Faber, H. de Waal, P. G. Kik, and A. Polman, Appl. Phys. Lett. **71**, 1818 (1997).
[3] A. Polman and F. C. J. M. van Veggel, J. Opt. Soc. Am. B **21**, 871 (2004).
[4] F. Priolo, G. Franzò, D. Pacifici, V. Vinciguerra, F. Iacona, and A. Irrera, J. Appl. Phys. **89**, 264 (2001).
[5] F. Iacona, D. Pacifici, A. Irrera, M. Miritello, G. Franzò, F. Priolo, D. Sanfilippo, G. Di Stefano, and P. G. Fallica, Appl. Phys. Lett. **81**, 3242 (2002).
[6] H. S. Han, S. Y. Seo, and J. H. Shin, Appl. Phys. Lett. **79**, 4568 (2001); H. S. Han, S. Y. Seo, J. H. Shin, and N. Park, *ibid.* **81**, 3720 (2002).
[7] P. G. Kik and A. Polman, J. Appl. Phys. **91**, 534 (2002).
[8] F. Gourbilleau, C. Dufour, M. Levalois, J. Vicens, R. Rizk, C. Sada, F. Enrichi, and G. Battaglin, J. Appl. Phys. **94**, 3869 (2003).
[9] F. Gourbilleau, M. Levalois, C. Dufour, J. Vicens, and A. Rizk, J. Appl. Phys. **95**, 3717 (2004).
[10] C. Ternon, F. Gourbilleau, X. Portier, P. Voivenel, and C. Dufour, Thin Solid Films **419**, 5 (2002).
[11] N. Daldosso, M. Melchiorri, F. Riboli, M. Girardini, G. Pucker, M. Crivellari, P. Bellutti, A. Lui, and L. Pavesi, J. Lightwave Technol. **22**, 1734 (2004).
[12] W. J. Miniscalco, J. Lightwave, J. Lightwave Technol. **9**, 234 (1991); A. J. Kenyon, C. E. Chryssou, C. W. Pitt, T. Shimizu-Iwayama, D. E. Hole, N. Sharma, and C. J. Humphreys, J. Appl. Phys. **91**, 367 (2002).
[13] M. Wojdak, M. Klik, M. Forcales, O. B. Gusev, T. Gregorkiewicz, D. Pacifici, G. Franzò, F. Priolo, and F. Iacona, Phys. Rev. B **69**, 233315 (2004).
[14] N. Daldosso, D. Navarro-Urrios, M. Melchiorri, L. Pavesi, F. Gourbilleau, M. Carrada, R. Rizk, C. García, P. Pellegrino, B. Garrido, and L. Cognolato, Mater. Res. Soc. Symp. Proc. **832**, F11.3.1 (2005).
[15] D. Pacifici, G. Franzò, F. Priolo, F. Iacona, and L. Dal Negro, Phys. Rev. B **67**, 245301 (2003).
[16] M. A. Green, *Silicon Solar Cells* (University of New South Wales, Sydney, 1995), p. 48.
[17] W. Spitzer and H. Y. Fan, Phys. Rev. **108**, 268 (1957).